EFFECT OF SILICA ON DEPOSITION AND AGEING OF CALCIUM CARBONATE FOULING LAYERS

P. Besevic[1], S.M. Clarke[2], G. Kawaley[3] and D.I. Wilson[1,*]

[1] Department of Chemical Engineering and Biotechnology, University of Cambridge, Philippa Fawcett Drive, West Cambridge Site, Madingley Road, Cambridge, CB3 0AS, UK; *diw11@cam.ac.uk
[2] Department of Chemistry and BP Institute, University of Cambridge, Madingley Rise, Cambridge, CB3 0EZ, UK
[3] Mitsubishi Electric R&D Centre Europe BV, 17 Firth Road, Houston Industrial Estate, Livingston, UK, EH54 5DJ

ABSTRACT

The effect of silicon derivatives on calcium carbonate fouling on copper surfaces was studied using synthetic solutions of calcium carbonate precursors and sodium silicate. Speciation of the silicon-containing compounds present was not attempted. Solutions were recirculated through a simple co-current heat exchanger cell for periods up to 100 hours while solution chemistry and heat transfer performance were monitored. Deposit structure, thickness and mass were also investigated by independent methods. Deposition of carbonate was controlled by the concentration of calcium in solution, which decreased over time in these batch experiments. Once the bulk calcium concentration reached an equilibrium level, deposition stopped. In the absence of silica, the thickness, voidage and thermal resistance of the fouling layer decreased, which was shown to be caused by the transformation of the initially formed aragonite to the calcite polymorph. This transition was inhibited in the presence of silica, so that the deposit retained a more open and thermally resistant structure. The rate at which calcium was removed from solution was also inhibited in the presence of silica. The experiments provide insight into the process of ageing during crystallization fouling.

INTRODUCTION

A strict definition of 'water' is the liquid phase of the substance with chemical formula H_2O. However, when people refer to water colloquially, they are rarely referring to the pure liquid. In practice, most water worldwide exists as the solvent in a dilute solution containing dissolved minerals, and occasionally suspended particles. The fact that water can accommodate dissolved material under a set of conditions and precipitate them when heated gives rise to crystallisation fouling. Calcium carbonate is a commonly encountered foulant and deposits on heated surfaces owing to its inverse solubility behaviour (it becomes less soluble at higher temperature). Water which contains the precursors for calcium carbonate deposition is likely to contain other trace elements, especially ground water as it is generated by flow through complex geological systems. Certain geological systems contain siliceous rocks, which over long periods of time can introduce a minor 'silica' component to the water chemistry. In practice, it has been observed that fouling in heating, ventilation and air conditioning (HVAC) systems is worse in places where the local groundwater has a high silicon content (Kawaley, 2015), where the silicon can be present in a number of forms. In this paper, the term 'silica' is used to refer to all forms of silicon and its derivatives that may be present in solution. It is acknowledged that the term is sometimes reserved for the crystalline form SiO_2.

Hard water operating environments are problematic for the operation of heat exchangers in HVAC applications. The susceptibility of such units to fouling is important because domestic devices aim to require minimal maintenance. Knowledge of the mechanisms by which trace components, such as silica, can exacerbate or mitigate the effect of fouling is desired for developing more robust units.

In this paper, the amount of silica or its derivatives present in solution or as solid is quantified in terms of the amount of elemental silicon that is present. For instance, if a solution was prepared using 87 mg/l of Na_2SiO_3, there would be 20 mg/l of silicon in the solution, and the concentration of silica and/or its derivatives is quoted as 20 mg Si/L. The reason for this is that it is very difficult to know the exact speciation of siliceous material at any given point in time, whereas the amount of elemental silicon can be measured directly using techniques such as inductively coupled plasma-mass spectrometry (ICP-MS).

The solution chemistry of silica or siliceous species is complex. Iler's book (1979), published nearly 40 years ago, provides a comprehensive review of the behaviours of silica in solution. Since then, there has been a large amount of research on concentrated silica solutions used in sol gel fabrication methods for solid oxides (*e.g.* Singh *et al.* 2014). However, there has been comparatively little work published on the behaviour of silica in dilute solution, which is the regime of interest for this work.

Silica polymorphs have different solubility limits in water and there are kinetic limitations when transforming between polymorphs. The solubility limit for amorphous silica in water is ~200 mg Si/l at 20°C, whereas for quartz the solubility limit is ~6 mg Si/l. Typical silica concentrations for siliceous groundwater are 15-40 mg Si/l. It is assumed that silica in these water systems exists as tiny colloidal particles on the nanometre scale; Iler states that in order to fully dissolve and dissociate silica or a silicate to orthosilicic acid,

ISBN: 978-0-9984188-0-3; Published online www.heatexchanger-fouling.com

$SiOH_4$ in its protonated form, a very low pH is required (Iler, 1979). Silica is a prograde solubility material; this means that as temperature increases, its solubility limit increases. This makes the idea that silica should affect deposition on heated surfaces somewhat counter-intuitive. Although most silica material becomes more soluble with temperature, it is also known that some silicates display retrograde solubility, in particular certain magnesium silicates (Brooke, 1984).

Silica fouling is a well-known phenomenon in power plants, where the pressure and temperature in turbine systems are considerably higher than for HVAC systems. In power plants silica deposits predominantly as alpha quartz and amorphous silica (Straub & Grabowski, 1945). Silica fouling problems have also been reported in reverse osmosis (RO) membranes where it deposits as amorphous silica (Ning, 2003). This paper focuses on mains hard water solutions containing a modest amount of dissolved silica (<40 mg/l Si) in combination with the precursors for calcium carbonate deposition which cause deposition in heaters operating with surface temperatures below 100°C and modest operating pressures. These conditions differ from those in the majority of the literature that discusses fouling problems with silica, particularly in geothermal power stations (*e.g.* Hernandez-Galan and Plauchau, 1989).

A second non-standard aspect of this fouling study is the use of copper substrates. There are many examples of studies of calcium carbonate fouling on stainless steels, particularly SS316 (*e.g.* Paakkonen *et al.* 2009), but there is little in the literature on copper even though it is commonly used in HVAC devices due to its high thermal conductivity and favourable chemical behaviour.

There are three sets of parameters that pertain specifically to the fouling material that determine its effect on heat transfer. Firstly, the amount of material that is deposited; it is reasonable to expect that more deposition in terms of mass deposited results in a greater thermal resistance due to fouling. Secondly, the composition of the material that deposits; thermal resistance due to fouling is a function of the thermal conductivity of the fouling material, which is a value determined by its composition. The final parameter, which is not always studied rigorously, is the physical structure of the fouling material. With mineral scales, the water has a lower thermal conductivity than the solid phase so a high voidage microstructure will give a larger thermal resistance, assuming that the liquid in the void spaces is largely stagnant so that there is little convective heat transfer in the deposit.

This paper examines the effect of low concentrations of silica on calcium carbonate fouling, where the carbonate is depositing on copper substrates. As well as monitoring the thermal performance of the system and measuring the amount of material that deposits, care was taken to characterise the structure of the deposit to build an understanding of the factors that affect thermal performance.

EXPERIMENTAL METHODS

Deposition of Fouling Material

A simple, co-current heat exchanger was used to generate fouling deposits. A flat copper substrate was located between two recirculating flows, illustrated in Figure 1(*a*). A hot water heater/recirculator provided the utility to heat the substrate surface. The cold stream (process stream) was a synthetic aqueous solution of known composition which was recirculated from a stirred 4 l reservoir. The exposed area of the copper substrate was 12 mm wide, 140 mm long with semi-circular ends, shown in Figure 1(*c*).

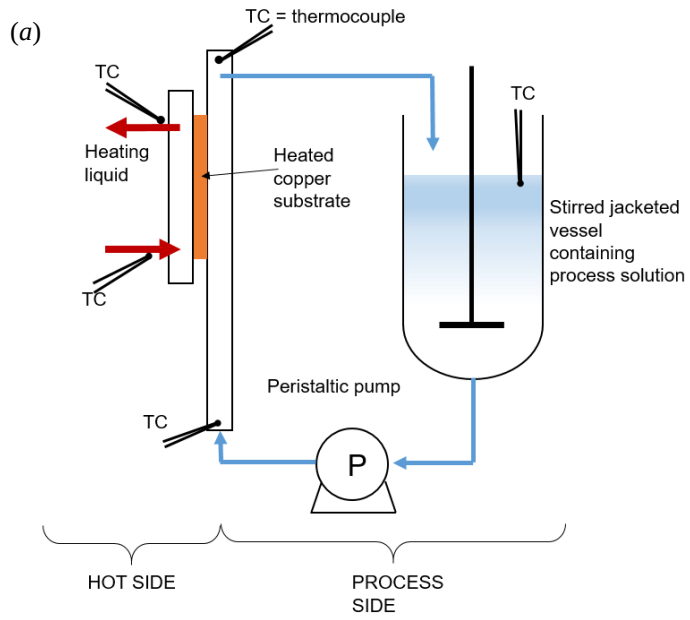

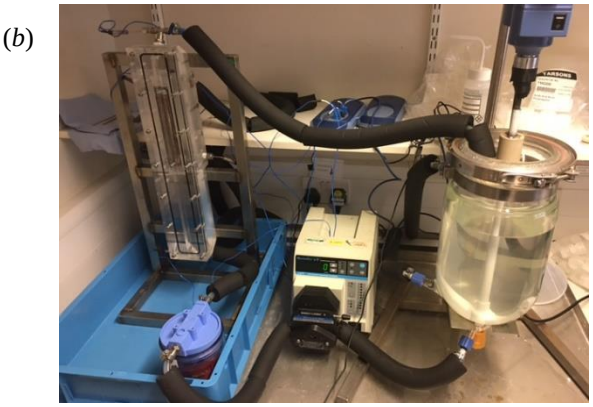

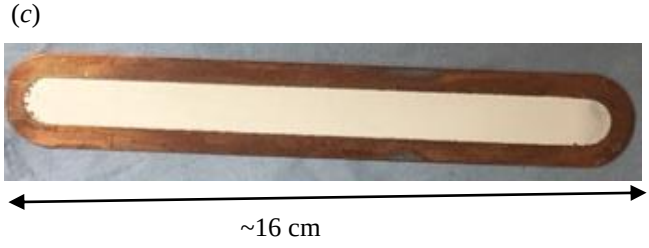

Figure 1. Fouling cell; (*a*) Schematic; (*b*) Photograph of fouling cell; (*c*) Photograph of test plate with deposit.

Inlet and outlet temperatures were measured using Type T thermocouples for both streams. The flow rate was maintained constant and logged on a PC: enthalpy balances gave the instantaneous heat duty, overall heat transfer coefficient, U, and thermal resistance due to fouling, R_f. For all the tests reported here, the flow rate of the process stream was 1.5 l/min and the channel dimensions were 12 mm wide

ISBN: 978-0-9984188-0-3; Published online www.heatexchanger-fouling.com

and 6 mm high, corresponding to an inlet Reynolds number of approximately 4,500.

The photograph of the apparatus in Figure 1(b) shows that the cell walls are transparent so that photographs could be taken periodically to monitor the evenness of deposition. During a fouling run the cell was contained within a light-tight box to control illumination. The fouling cell operates in batch mode, the advantages of this approach being the ability to control the composition of the process solution at the start of the experiment and the ability to maintain a comparable flow rate to an HVAC unit for a sustained time period.

All solutions reported in this paper contained 200 mg/l Ca. They were prepared by mixing $CaCl_2.6H_2O$ (Fisher Scientific) and $NaHCO_3$ (Fisher Scientific) in RO water to ensure that each solution contained Ca and sufficient CO_3^{2-} to form $CaCO_3$. Sodium silicate, Na_2SiO_3 (Sigma Aldrich), was added to some solutions. The solutions were well shaken and allowed to rest to ensure that all of the material added had sufficient time to dissolve or disperse. In this paper, calcium carbonate hardness is defined in terms of the amount of dissolved calcium and similarly silica hardness is defined in terms of amount of dissolved and dispersed silicon. The pH of the solutions ranged from 7.5 – 8.0.

Analysis of Process Solution and Fouling Material

Aliquots were taken from the reservoir periodically to measure the amount of material leaving the solution. These aliquots were analysed using ICP-MS. The deposited material on the copper substrate was dissolved in strong acid (2M HCl) and analysed using ICP-MS in order to quantify the amount of deposit. For systems involving silica the protocol for preparing solutions for ICP analysis was more complicated because the only solution that reliably dissolves silica is $HF_{(aq)}$ A further complication identified during this study was that when analysing mixed calcium carbonate-silica systems, an insoluble precipitate of CaF_2 forms when calcium carbonate reacts with HF. Therefore, a series of washes using HCl and HF was devised to ensure all deposited silica and calcium carbonate was measured.

The change in composition of the process stream over time gives an important insight into the kinetics of deposition and approach to equilibrium. The measurement of the amount of material deposited on the copper substrate allows the voidage of the layer to be evaluated and to perform a mass balance on the material leaving solution, to check whether carbonate deposits elsewhere in the system.

Scanning electron microscopy (SEM) on the fouling material indicated the shape, size and packing of the deposited crystallites. Images were taken using an FEI Quanta SEM under low vacuum: this obviated the need to coat the samples using a conductive material such as gold. The samples were analysed for elemental composition and mapped using energy dispersive x-ray spectroscopy (EDS) using a Bruker Quantax EDS probe.

A Micro-Epsilon confocal thickness sensor was used to measure the thickness of deposited layers. Line scans were taken across the fouling layer in several places to confirm that the thickness of the layer was broadly uniform across its surface.

RESULTS AND DISCUSSION

Systems without Silica

Figure 2 shows the evolution of the overall heat transfer coefficient, U, and thermal resistance due to fouling, R_f, for a solution containing 200 mg/l Ca and no silica. There is a modest change in U with respect to time, and a more marked change in R_f. Initially R_f increases with time, as expected, but after about 35 hours it decreases. The magnitude of R_f is quite small: the fouling layers deposited in this experiment are not very thick.

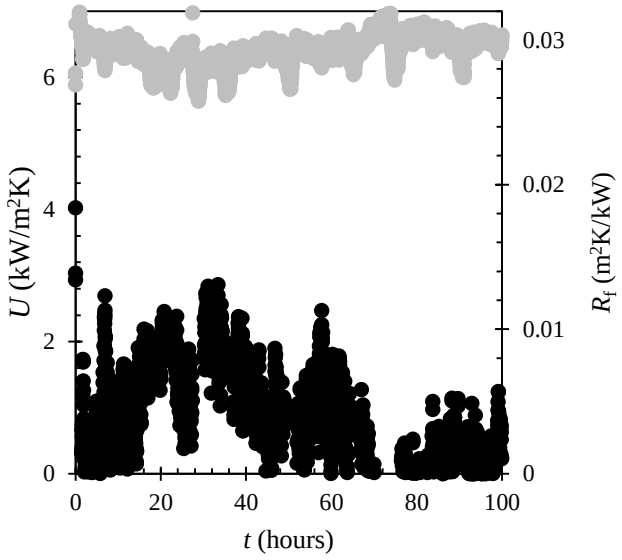

Fig. 2 Heat transfer data for system containing 200 mg/l Ca, Re ~ 4400, T_s ~ 63°C; Grey symbols - U, left axis: black symbols - R_f, right axis; Cold stream temperature ~ 42°C, Hot stream temperature ~ 79°C.

Figure 3 shows the concentration of calcium in solution over the first 40 hours of the test. The dashed horizontal line on the plot shows the saturation concentration of calcium at the surface temperature of the copper substrate, T_s, which was around 63°C in this case. This was calculated by solving the set of coupled equilibria described by Plummer and Busenburg (1982) for the deposition of calcium carbonate using a MATLAB script. The concentration of calcium approaches the surface saturation value steadily and reaches it after approximately 35 hours, which corresponds to when R_f stops increasing. The remainder of the test in Figure 2 corresponds to extended operation with heat transfer but little further deposition. The Biot number is less than 0.1, so the temperature in the deposit is not very different from the initial, clean conditions.

Figure 3 shows that the [Ca]-t data, when written in terms of concentration driving force for crystallisation, Γ = [Ca]-[Ca]$_s$, exhibits first order kinetics. This suggests that deposition is mass transfer controlled, as calcium carbonate crystallization is reported to be second order in concentration driving force (Segev *et al*., 2011).

The amount of inorganic carbon present in solution was also measured and from this the CO_3^{2-} concentration could be calculated using the system of equilibria described by Plummer and Busenburg (1982). [CO_3^{2-}] was ~5x10^{-5} mol/l which is much less than [Ca] at the start of the experiment

ISBN: 978-0-9984188-0-3; Published online www.heatexchanger-fouling.com

($5x10^{-3}$ mol/l). [CO_3^{2-}] did not vary much over time. CO_3^{2-} was/is replenished in the system by the deprotonation of HCO_3^- ions. The system was not perfectly isolated so some carbon dioxide could be absorbed from the atmosphere over time. This accounted for the modest change in pH (from approximately 8 to around 7.5).

More experiments were carried out to investigate the change in R_f in Figure 2. One experiment was curtailed after about 40 hours (all other operating parameters being identical). The thermal data collected for this period of time were essentially identical to Figure 2. The amount of material deposited on the copper substrate is reported in Table 1.

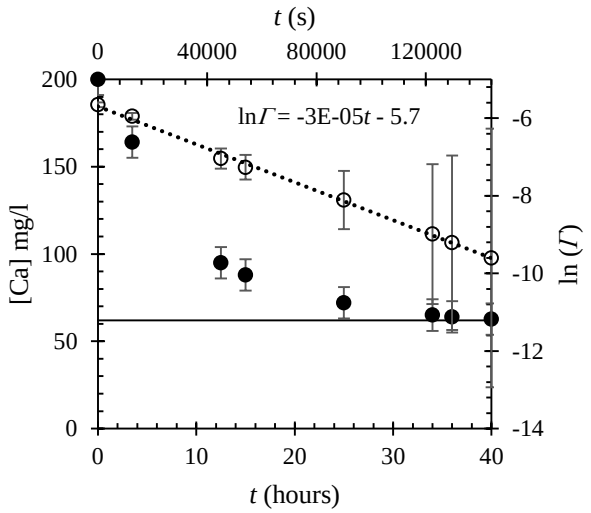

Fig. 3 Concentration of Ca in process stream reservoir for the first 40 hours of the test in Fig. 2. Horizontal solid line: calcium carbonate saturation concentration at T_s. Solid symbols – [Ca]; open symbols - concentration driving force for deposition, Γ, plotted on logarithmic scale. Dashed locus shows first order decay model fitted to Γ data with t in seconds.

Table 1. Amount of material deposited for long and short fouling runs with 200 mg/l Ca, Re ~ 4400, T_s ~ 63°C.

Test duration	Amount of Ca deposited
40 hours	542±17 mg
100 hours	546±17 mg

Within experimental error, the same amount of material was deposited after 40 and 100 hours, confirming that the formation of new deposit stopped when the concentration driving force reached zero.

One would normally expect R_f to increase with time and reach an asymptote as the process solution is depleted of calcium; this is not evident in Figure 2. Five possible mechanisms were postulated to account for this behaviour; (i) material is removed with time due to shear at the surface; (ii) deposition makes the channel narrower, thereby increasing the Reynolds number and improving the process-side film heat transfer coefficient; (iii) the roughness of the deposit changes with time, thereby increasing turbulence at the surface and again improving heat transfer, (iv) a change in thickness of the deposit due to physical mechanisms, such as the stresses induced by the flowing process stream compacting the crystallites; (v) the crystal structure of the deposit changes with time due to recrystallisation of the deposit. Mechanism (i) is discounted because the stresses imposed by flowing fluid in this system are small and sloughed material is not recovered at the end of a test.

Mechanisms (ii) and (iii) require knowledge of the deposit thickness and summaries of confocal thickness measurements are given in Table 2. The change in channel depth is modest so mechanism (ii) can be discounted. Moreover, the layer thickness and roughness decreased over time, indicating that the fouling layer somehow changes its microstructure between 40 and 100 hours.

The voidage of the deposit, ε, was calculated by dividing the volume of pores or voids by the total volume of the deposit. The total volume, V_T, of the deposit can be calculated using the average deposit thickness, δ, in Table 2 and the surface area for deposition, which is known (0.0017 m^2). The pore volume was calculated by subtracting the volume of solid material from V_T. The volume of solid material can be estimated by dividing the mass of deposit, m (see Table 1) by the skeletal density of calcium carbonate, ρ_{CaCO3}, via:

$$\varepsilon = (V_T - m/\rho_{CaCO3}) / V_T \quad [1]$$

Table 2. Effect of run time on deposit thickness, δ, and roughness, R_q. Test conditions: 200mg/l Ca, Re ~ 4400, T_s ~ 63°C. t = 0 corresponds to the copper substrate.

Run time hours	δ µm	R_q µm	Voidage, ε -
0	0	64±4	-
40	210±9	132±11	0.48
100	142±7	87±8	0.21

Insight into the microstructure was provided by estimating the voidage of the deposit. Treating the deposit as a slab of uniform thickness, δ, R_f is given by:

$$R_f \approx \delta/\lambda_f \quad [2]$$

where λ_f is the thermal conductivity of the fouling layer. λ_f is assumed to be related to the thermal conductivity of a fully dense crystal and the voidage, ε, by a law of mixtures:

$$\lambda_f = \lambda_{crystal} (1- \varepsilon) + \lambda_{water} \varepsilon \quad [3]$$

where the subscripts refer to the phase. The voids in the deposit are occupied by solution, which has a lower thermal conductivity than the solid crystal. The mass of deposit per unit area, m_a, is given by:

$$m_a = \delta \rho \quad [4]$$

where ρ is density. Substituting [3] and [4] into [2] yields the following relationship between R_f and voidage:

$$R_f \approx m_a/(\rho_{water}\varepsilon + \rho_{crystal}(1- \varepsilon)) \times ((1- \varepsilon)/\lambda_{crystal} + \varepsilon/\lambda_{water}) \quad [5]$$

Figure 4 shows the prediction of this model for the case where m_a is fixed. The thermal performance is strongly sensitive to the amount of voids in the structure. There is an order of magnitude difference in thermal performance for the range of values considered here, and notably a decrease of about 50% between the ε values obtained for the deposit at different times in Table 2. This corroborates the thermal resistance change in Figure 2 and reaffirms that the deposit structure, particularly its voidage, is important.

The above analysis only considers conductive heat transfer through the deposit. This is reasonable given the data in Figure 2 and Tables 1 and 2, where a more open physical structure gives poorer thermal performance. A more rigorous analysis would consider contributions from convective heat transfer associated with liquid flowing through pores in the deposit, which may enhance heat transfer in high voidage materials. Convective heat transfer through porous fouling layers has been considered by Xiao *et al.* (2017).

The SEM images of samples retrieved from the fouling rig in Figure 5 show that the microstructure of the fouling layer evolved between 40 and 100 hours. There is evidence of recrystallisation of material. At 40 hours, Figure 5(*a*), the material at the surface consisted of small crystals, almost all needle shaped. This is characteristic of the aragonite polymorph of calcium carbonate. Aragonite is not the most thermodynamically stable form of calcium carbonate under the conditions in this experiment – calcite is - but the energy barrier for heterogeneous nucleation of aragonite is often lower than for calcite. Noda *et al.* (2013) studied the deposition of calcium carbonate on copper and reported a mixture of aragonite and calcite. After 100 hours, Figure 5(*b*), the microstructure of the crystals at the surface has changed. There are still many needle shaped crystals, but they appear to be finer than in Figure 5(*a*). Moreover, there are now crystals with shapes with a lower aspect ratio which are consistent with the morphology of calcite.

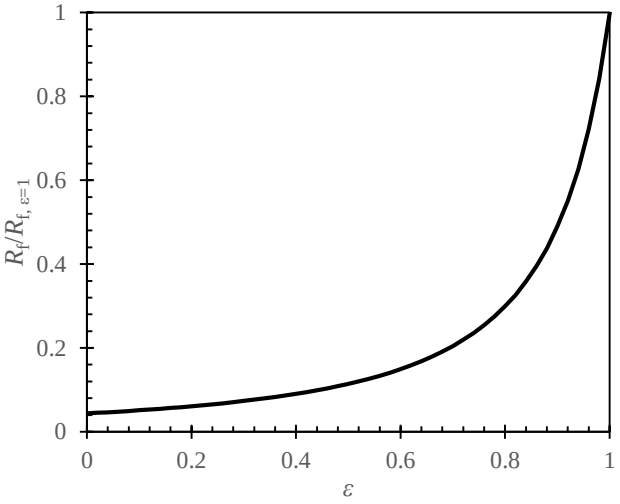

Figure 4: Plot of Equation [4], comparing normalised thermal resistance due to fouling, $R_f/R_{f,\varepsilon=1}$, and voidage, ε, for a fixed mass of deposit per unit area. $\rho_{crystal}$ = 2700 kg/m^3, λ_{water} = 0.65 W/m K and $\lambda_{crystal}$ = 5.6 W/m K. The two extremes, ε = 0 and ε = 1, represent a solid, fully dense crystal and a highly porous gel, respectively.

The phase transformation between aragonite and calcite is diffusional, which means that aragonite crystals have to dissolve to form calcite; this is consistent with the images in Figure 5. The needle shaped crystals are similar in length in both images but are finer in Figure 5(b) than in Figure 5(a), indicating that material is lost from the faces of the aragonite needle to forms the calcite rhomb. This evidence suggests that the decrease in thermal resistance due to fouling is caused by the recrystallisation and transformation of the fouling layer. It has been observed in these tests because deposition of fresh material has been interrupted by Γ approaching zero: the solution is effectively saturated in calcium carbonate, facilitating the diffusion of the ions.

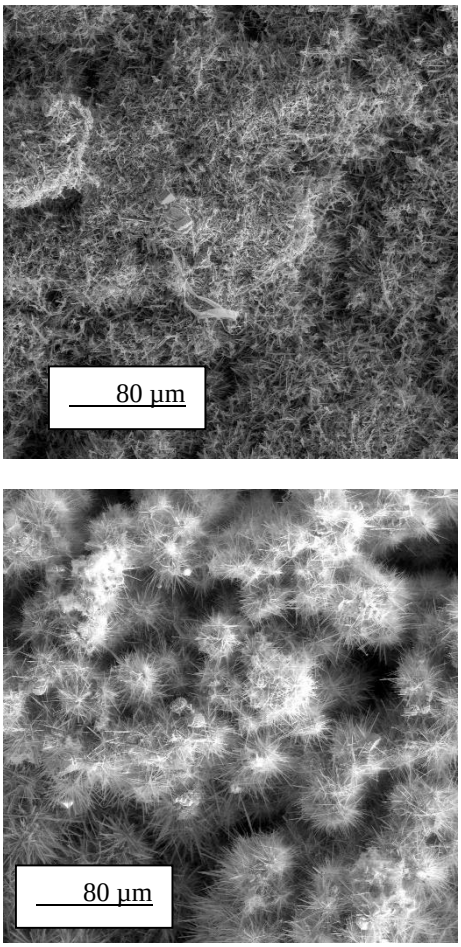

Figure 5: Secondary electron images of surface of fouling deposit after (a) 40 hour and (b) 100 hour runs. Conditions: 200 mg/l Ca, Re ~ 4400, T_s ~ 63°C.

Ageing

Combining the data from Figure 2, Table 2 and Figure 5, it is clear that an ageing process has taken place, with ageing defined as the transformation of fouling material after its initial deposition. It is rare for clear, quantitative data about ageing of fouling material to be reported, typically due to the long timescales required for many types of fouling material to age.

Respondents to a self-assessed survey at the Heat Exchanger Fouling and Cleaning Conference in 2009, a

group considered representative of engineers working in fouling, agreed that ageing was the least well understood of the sequential events in fouling as originally described by Epstein (Wilson, 2009, Epstein, 1983). In this experiment, a stage was reached after about 30 hours (see Figures 2 and 3) where deposition had essentially been 'switched off' due to running a batch experiment with a relatively low volume. After supersaturated calcium had been removed from the solution, the only ongoing fouling process was ageing. To the authors' knowledge (and they would be delighted to be corrected on this), this is the first reported example where ageing has been isolated as a fouling process experimentally, and where ageing has been systematically studied and demonstrated in terms of heat transfer performance, macrostructure (thickness) and microstructure.

Systems with Silica

Figure 6 shows the evolution of overall heat transfer coefficient over time for a similar system to that in Figure 2, but with 20 mg Si/l in solution. The result is quite different as the fouling resistance increases with time and reaches an asymptotic value. The noticeable perturbations in the *U*-*t* and thus R_f-*t* data are associated with thermal events when the heating utility was topped up with water. The cause of these artefacts is the subject of ongoing investigation.

Figures 7 and 8 present the associated evolution in bulk solution composition for this fouling run. Comparing Fig. 7 with Fig. 3 indicates that less calcium deposited in the presence of silica and this was confirmed by the deposit analysis in Table 3. The fouling resistance after 100 hours, of around 0.16 m^2K/kW, is of similar magnitude to the maximum reached in Fig. 2 before deposition stopped and ageing dominated

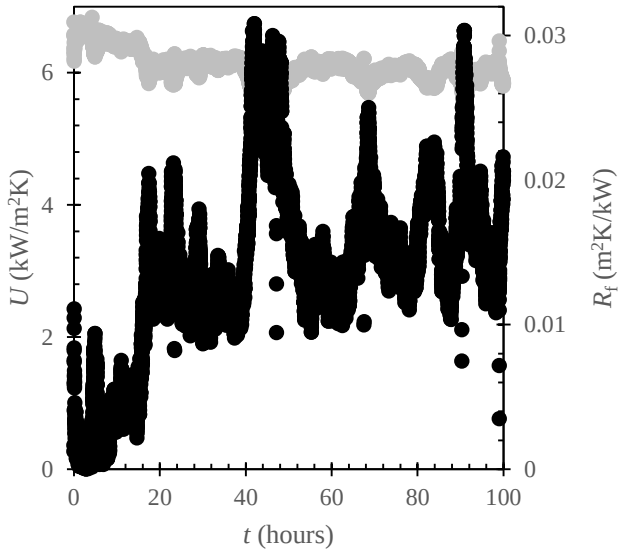

Fig. 6 Heat transfer data for system containing 200 mg/l Ca, 20 mg Si/l, *Re* ~ 4400, T_s ~ 63°C; Grey symbols - *U*, left axis: black symbols - R_f, right axis; Cold stream temperature ~ 42°C, Hot stream temperature ~ 79°C.

Table 3. Amount of material deposited for long fouling run with 200 mg/l Ca, 20 mg Si/l, *Re* ~ 4400, T_s ~ 63°C.

Test duration	Amount of Ca deposited	Amount of Si deposited
40 hours	405±14 mg	17±3 mg
100 hours	482±14 mg	19±3 mg

The calcium concentration data again gave a good fit the first order kinetic model in concentration driving force, *viz*.

$$\ln(\Gamma) = -k_{m,\,eff}\,t + \ln(\Gamma)_{t=0} \qquad [6]$$

where $k_{m,eff}$ is the effective mass transfer coefficient. Comparing the $k_{m,eff}$ values between Figures 3 and 7, it is apparent that calcium carbonate deposition in the presence of silica is slower (without Si, 3×10^{-5} s^{-1}; with Si, 5×10^{-6} s^{-1}). However, the thermal resistance due to fouling resistance is greater in the presence of silica.

Figure 8 shows the concentration of silica in the process stream. Some silica is removed from the process solution early in the experiment, probably due to adsorption to surfaces in the test rig including the fouling layer. The concentration of silica remains effectively constant thereafter: there is no progressive decay associated with deposition of silica. Similarly, the thickness and roughness measurements after 40 and 100 hours in Table 4 show no appreciable change. These data show that the ageing observed in the system without silica is not observed when silica is present.

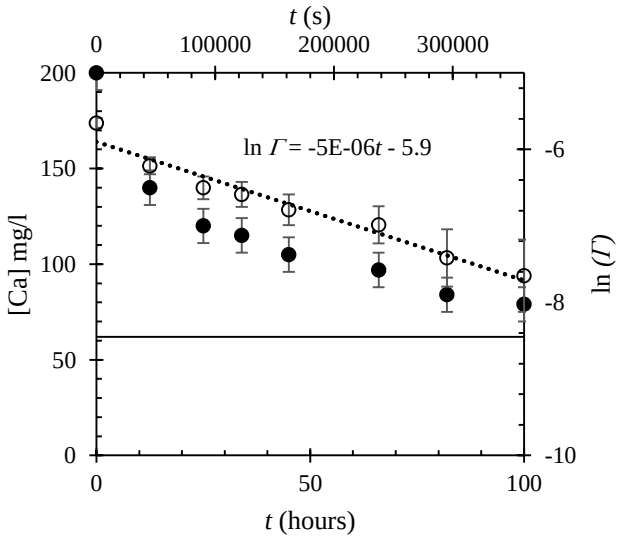

Fig. 7 Concentration of calcium in the reservoir of the fouling cell with over time for test in Fig. 6. Closed symbols – [Ca]; open symbols – Γ. Horizontal solid line indicates $[Ca]_{sat}$ for the surface temperature in this test. Dotted line shows fit to Equation [6].

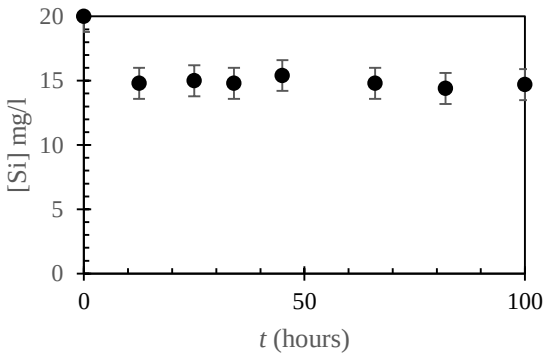

Fig. 8 Concentration of Si in reservoir of fouling cell over time for test in Fig. 6. Initial [Si] = 20 mg Si/l.

Table 4. Effect of run time on deposit thickness, δ, and roughness, R_q. Test conditions as in Table 3. t = 0 corresponds to the copper substrate.

Run time hours	δ µm	R_q µm	Voidage, ε -
0	0	64±4	-
40	243±9	155±8	0.62
100	248±12	164±7	0.56

Deposit microstructure

Figure 9 shows micrographs comparing deposits generated without silica after 40 and 100 hours, and one generated in the presence of silica after 100 hours. The system with silica has larger needle-shaped crystals at the surface than the system without silica. After 100 hours, the needles at the surface of the sample are larger and coarser again; this is likely due to normal Otswald ripening affecting crystal growth. The needle shape is retained over time: it is harder to pack needles efficiently than shapes with lower aspect. This means that the microstructure is more open and porous, and results in different heat transfer performances evident in Figures 2 and 6 for systems with and without silica, respectively.

Figure 10 shows EDS images which allow locations of silicon atoms to be identified. Figure 10(*a*) shows an image taken of the surface of a deposit and this shows qualititatively that there is a fairly even distribution of Si across the surface of the sample. Figure 10(*b*) shows a cross-section where the substrate and deposit was mounted in resin, cut and polished. It is clear that silica interacts with the copper surface and the surface of the calcium-based crystallite. Adsorption of silica to the copper substrate at the start of the experiment would explain some of the decrease in concentration in Figure 8.

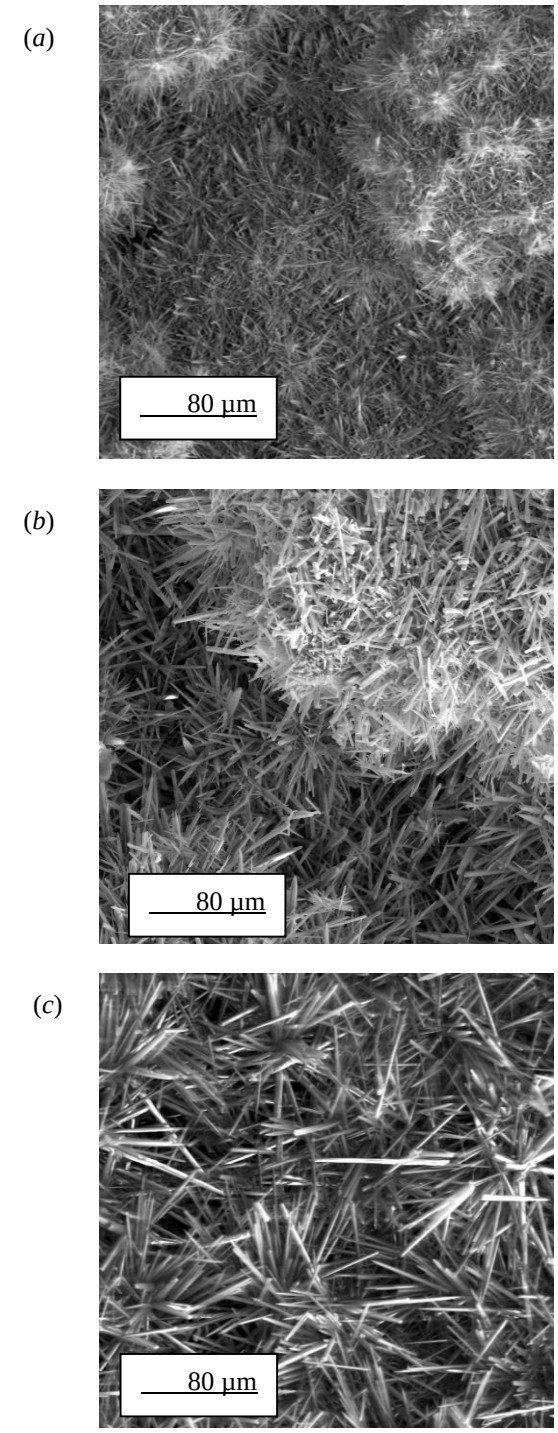

Figure 9: Secondary electron images of surface of fouling material. (a) 200 mg Ca no Si, 40 hours; (*b*) 200 mg Ca 20 mg/l Si, 40 hours; (*c*) 200 mg Ca, 20 mg/l Si, 100 hours.

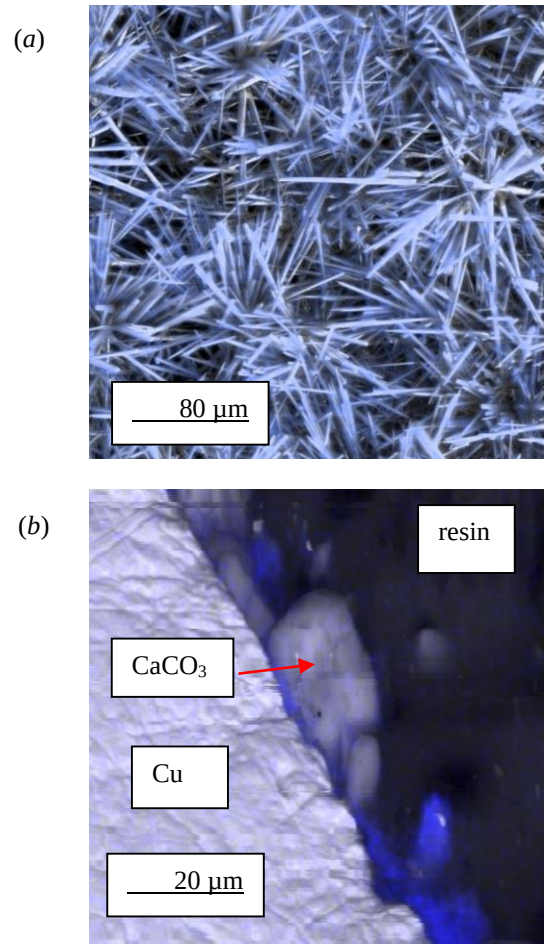

Figure 10: EDS maps of deposits generated from 200 mg/l Ca, *Re* ~ 4400, 20 mg/l Si, T_s ~ 63°C; blue represents location where Si is present; (*a*) map of deposit top surface; (*b*) depth profile of deposit and test plate mounted in resin and cross-sectioned.

Figure 10 gives some clues about the mechanism by which silica affects the ageing of calcium carbonate. Silica will not go into solid solution with calcium carbonate at the pressure and temperature conditions involved in these tests. It is likely to be a surface effect rather than a bulk effect since silica cannot easily incorporate into calcium carbonate crystal structures. Since needle shaped crystals (aragonite) can, and do, grow, and the concentration of silica does not change markedly, this suggests that a passivating layer of silica completely preventing crystal growth does not form on the aragonite surface. The effect of silica on ageing of caclium carbonate fouling material is hypothesised to arise from silica affecting the nucleation of the calcite phase, hampering the polymorph transition. In an x-ray diffraction study of homogenous nucleation of calcium carbonate, Kellermeier *et al*. (2013) found that at elevated temperatures silica stabilised the aragonite phase. The above results are broadly consitent with their finding.

It should be noted that this study considered fouling on a substrate with synthetic waters containing only the precursors for calcium carbonate deposition and silica. Real systems are more complex, and other trace elements can have differing effects. For instance, phosphate ions stabilise the calcite phase (Noda *et al.*, 2013). Further work is required to establish the interactions between different species.

Most of the imaging presented here considered the fluid-deposit interface. In a real deposit, the material will be subject to different ageing timescales, and it would be good to augment this information by probing the morphology of crystals deposited at different locations within the deposit, and in contact with the substrate surface. A good technique to probe this would be X-ray tomography, although a high energy beamline would be necessary due to the high X-ray absorbance properties of the copper substrate.

CONCLUSIONS

Trace components are known to affect hard water fouling. Silica has been demonstrated to affect the ageing behaviour of calcium carbonate deposits generated on copper surfaces at temperatures representative of those found in commercial HVAC systems. In the absence of silica, ageing has been shown to have a mitigating effect on fouling and reduced the thermal resistance of a deposit. Silica has been shown to hinder the transformation from aragonite to calcite and the associated rearrangement of deposit microstructure. The work represents a systematic experimental study of ageing.

ACKNOWLEDGEMENTS

The authors gratefully acknowledge financial support and permission to publish from Mitsubishi Electric Corporation. Thanks are due to Dr Giulio Lampronti and Dr Jason Day from the Department of Earth Sciences, for help with electron microscopy and ICP-MS analysis, and to Andy Hubbard, Department of Chemical Engineering and Biotechnology, for construction, modification, and maintenance of the fouling rig.

NOMENCLATURE

Roman

C_{bulk}	Bulk concentration, mol/m^3
C_{sat}	Saturation concentration, mol/ m^3
$k_{m,eff}$	Effective mass transfer coefficient, m/s
m	Mass of deposit, kg
m_a	Mass of deposit per unit area, kg/m^2
R_f	Thermal resistance due to fouling, m^{2}K/W
R_q	Roughness (root mean squared), µm
t	Time, s
T	Temperature, °C
U	Overall heat transfer coefficient, W/m^{2}K
V_T	Total volume of deposited material, m^3

Greek

δ	Thickness of fouling layer, m
ρ	Density, kg/m^3
Γ	Concentration driving force, mol/m^3
λ	Thermal conductivity, W/m K

REFERENCES

Brooke, M. 1984, Magnesium silicate scale in circulating cooling systems, *Corrosion 84: The International Corrosion Forum Devoted Exclusively to the Protection and Performance of Materials*, Paper 327.

Epstein, N. 1983, Thinking about heat transfer fouling: a 5x5 matrix, *Heat Transfer Engineering*. Vol. 4, Issue 1, pp. 43-56.

Hernandez-Galan, J.L., Plauchau, A.L. 1989, Determination of fouling factors for shell and tube type heat exchangers exposed to Los Azufres geothermal fluids, Geothermics, Vol. 18, pp. 121-128.

Iler, R.K. 1979, *The Chemistry of Silica, Solubility, Polymerisation, Colloid and Surface Properties and Biochemistry of Silica*, 1st ed., Wiley, New York.

Kawaley, G. 2015, Personal Communication.

Kellermaier, M., Glaab, F., Klein, R., Melero-Garcia, E. Kunz, W. & Garcia-Ruiz, J.M. 2013, The effect of silica on polymorphic precipitation of calcium carbonate: an on-line energy dispersive x-ray diffraction (EDXRD) study, *Nanoscale*, Vol. 5, pp. 7054-7065.

Noda, S., Saito, T., Miya, K., Furukawa, S., Clarke, S.M., Wilson, D.I. 2013, The influence of phosphate on calcium carbonate formation in hard water, *Proc. Int. Conf. Heat Exchanger Fouling and Cleaning 2013*, Budapest, Hungary, pp. 165-169.

Ning, R.Y. 2003, Discussion of silica speciation, fouling, control and maximum reduction, *Desalination*, Vol. 151, pp. 67-73.

Paakkonen, T.M., Riihimaki, M., Puhakka, E., Muurinen, E., Simonson, C.J. & Keiski, R.L. 2009, Crystallisation fouling of $CaCO_3$ – Effect of bulk precipitation on mass deposition on the heat transfer surface, *Proc. Int. Conf. Heat Exchanger Fouling and Cleaning 2009*, Schladming, Austria, pp. 209-216.

Plummer, L.P. & Busenburg, E. 1982, The solubilities of calcite, aragonite and vaterite in CO_2-H_2O solutions between 0 and 90°C, and an evaluation of the aqueous model for the system $CaCO_3$-CO_2-H_2O, *Geochimica et Cosmochimcia Acta*, Volume 46, Issue 6, pp. 1011-1040.

Segev, R., Hasson, D. & Semiat, R. 2011, Rigorous modelling of the kinetics of calcium carbonate deposit formation, *AIChE Journal*, Vol. 58, Issue 4, pp. 1222-1229.

Singh, L. P, Bhattacharyya, S. K., Kumar, R., Mishra, G., Sharma, U., Singh, G. & Ahalawat, S. Sol-Gel processing of silica nanoparticles and their applications, *Advances in Colloid and Interface Science*, Vol. 214, pp. 17-37.

Straub, F. G. & Grabowski, 1945, Silica Deposition in Steam Turbines, *Transactions of the A.S.M.E*, pp.309-316.

Wilson, D. I. 2009, Preface, *Proc. Int. Conf. Heat Exchanger Fouling and Cleaning 2009*, Schladming, Austria, pp.vi-viii.

Xiao, J., Han, J., Zhang, F. & Chen, X. D. Numerical Simulation of Crystallisation Fouling: Taking into Account Fouling Layer Structures, *Heat Transfer Engineering*, vol. 38, pp. 775-785